and after surgery for all of them. For all patients, an open-door laminoplasty was performed, using 2 graft bones as spacers. The CT scans were obtained using a commercial CT system (LightSpeed, General Electric) with a slice thickness of 0.625 mm and a pixel size of 0.352 × 0.352 mm. The data were transferred via a DICOM (digital imaging and communications in medicine) network into a computer workstation, where image processing was performed using Virtual Place software (M series, Medical Imaging Laboratory). All protocols for this retrospective study were approved by our institution's review board.

Measurement of Progression and Volume Increase

Measurement of progression and volume increase consisted of 3 stages. First, each vertebra with OPLL was semiautomatically extracted at a specific threshold, using a process known as segmentation. A window width of 2000 HU and window level of 150 HU were used for the threshold, as has been done in earlier studies.[8,12] Second, the preoperative model of the vertebral body was superimposed over the postoperative model of the same vertebral body to obtain a matrix that represents migration. This superimposition is possible because after removal of the OPLL and opening of the lamina, the vertebral body can be regarded as a rigid body that does not vary from before surgery to after surgery. By this matrix, the OPLL attached to the vertebra was accurately superimposed (Fig. 1). Third, the progression length and volume increase between preoperative OPLL and postoperative OPLL was assessed with the original digital viewer (Orthopedic Viewer, Osaka University). Progression was visualized in color-coded contour at 0.5- or 1-mm intervals on the bone surface for better understanding. In measuring OPLL volume, it was difficult to determine the boundary between the OPLL and the vertebral body. Therefore, preoperative and postoperative OPLL models were extracted from the superimposed vertebrae in the same margin bounded by the rectangle, with bilateral inflection points between the vertebral body and pedicle as vertices (Fig. 2). The expansion rate (volume increase divided by prevolume) was also assessed.

Accuracy of Voxel-Based Registration

Voxel-based registration is a method for determining the relative positions of 3D models at different coordinates, using a corresponding method that is based on the correlation between CT values of each voxel.[9] This calculation is performed using software, and the relative positions are represented as a matrix. This matrix is converted to 6 df by Euler angles, with the sequence of yaw (Y), pitch (X), roll (Z), and translations, using a previously defined coordinate system[9] (Fig. 1). We performed in vitro validation of the accuracy of our experimental CT method for the cervical spine using fresh-frozen vertebrae. More than 8 tantalum beads with a radius of 1.0 mm were implanted in the vertebrae. Subsequently, CT scans were obtained 8 times in different positions with the same imaging parameters. Each vertebra was then superimposed by voxel-based registration. The true value of the

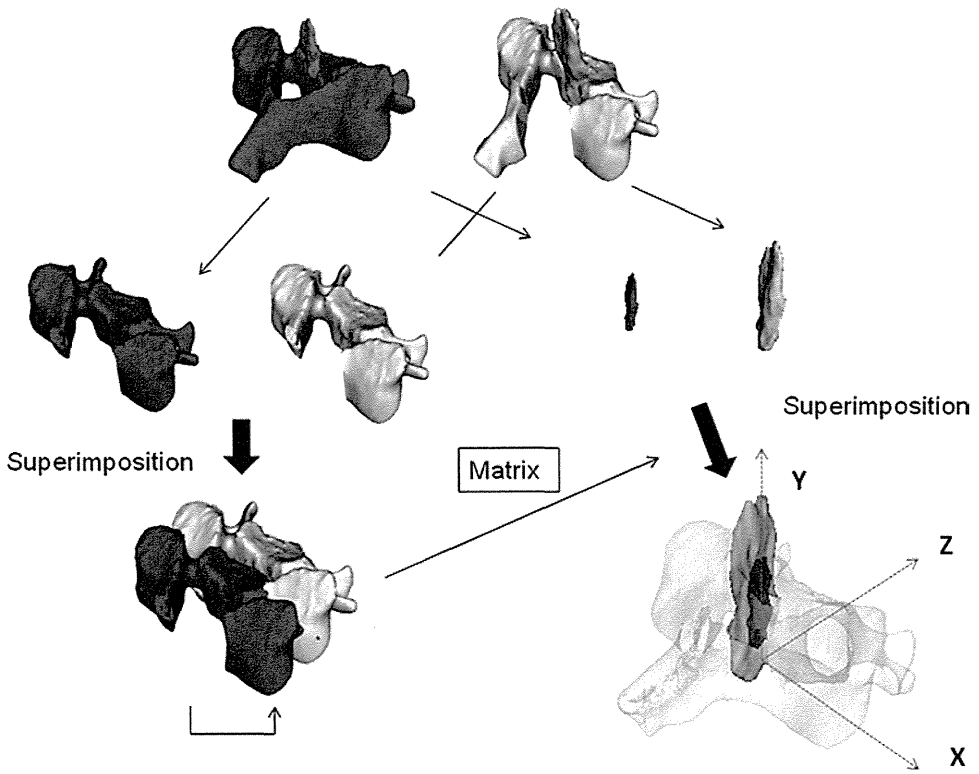

Fig. 1. Superimposition of OPLL by voxel-based registration. Three-dimensional models of OPLL before and after surgery were segmented together with the vertebral bodies. They were superimposed on the matrix derived from voxel-based registration of the vertebral bodies. This matrix is converted to 6 df by Euler angles, with the sequence of yaw (Y), pitch (X), roll (Z), and translations.

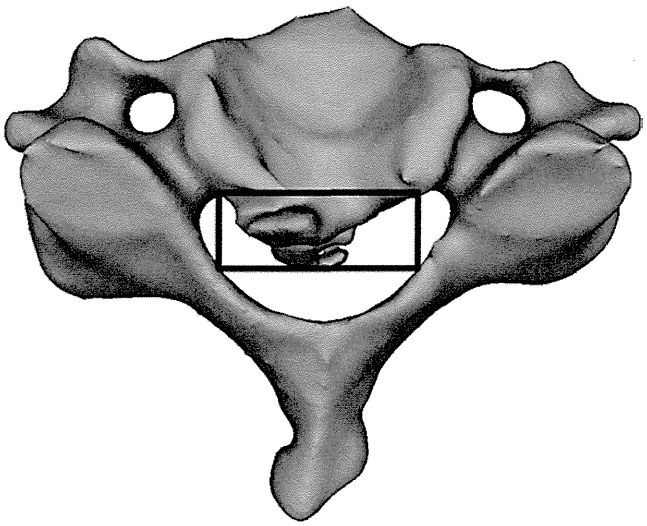

FIG. 2. The volume of OPLL was defined as the area bounded by the rectangle.

migration was measured by marker-based registration, providing gold-standard data. Accuracy was defined as the closeness to the true value; the RMSE was assessed.

Reproducibility of Volume Measurement

To assess reproducibility of measurement of OPLL volume, 3 observers measured the volume of 10 OPLL segments twice with 1 week elapsing between each measurement. Intraobserver and interobserver ICC, RMSE, and CV were assessed.

Results

Clinical Data

The mean patient age was 63 years (range 43–71 years), and the mean duration of follow-up monitoring was 3.1 years (range 2.1–3.8 years). The mean score on the Japanese Orthopaedic Association scale was 8.5 before surgery and 15.6 after surgery; the maximum possible score is 17. All patients experienced functional improvement after surgery. Four of the 5 patients had a mixed type of OPLL, and 1 had a localized type of OPLL (Table 1).

Progression of OPLL

Ossification of the posterior longitudinal ligament progressed 0.5 mm or greater in all patients. The average maximum progression length was 4.7 mm, and the progression rate was 1.5 mm/year (Table 1). The maximum progression occurred in the youngest patient (Case 1). Ossification of the posterior longitudinal ligament tends to grow actively around intervertebral areas and less in vertebral areas (Figs. 3 and 4).

Volume Increase of OPLL

The mean volume increase was 1622 mm^3 per patient, and the mean expansion rate was 37% during the follow-up period. The mean volume increase rate was 484 mm^3/year (Table 1).

Accuracy of Voxel-Based Registration and Reproducibility of Volume Measurement

The RMSE was 0.19° in flexion-extension, 0.13° in axial rotation, 0.21° in lateral bending, 0.13 mm in lateral translation, 0.15 mm in superoinferior translation, and 0.31 mm in anteroposterior translation (Table 2).

For intraobserver reproducibility of the volume measurement, the mean ICC, RMSE, and CV were 0.987, 16.0 mm^3, and 1.7%, respectively (Table 3). For interobserver reproducibility, the mean values were 0.968, 33.1 mm^3, and 3.4%, respectively (Table 4).

Illustrative Cases

Case 1

This 43-year-old man presented with a mixed type of OPLL. Before surgery, a plain lateral radiograph showed a continuous type of OPLL at the C2–3 level; however, the extent of OPLL at the C4–5 level was unclear (Fig. 3). Before surgery, the CT model clearly revealed a segmental type of OPLL at C-4, C-5, C-6, and C-7 (Fig. 4). Four years after laminoplasty, growth was apparent on radiographs; however, quantitative changes were unclear, especially at the levels of C-6 and C-7. The postoperative CT model revealed that the C3–4, C4–5, and C5–6 intervertebral spaces were bridged by growing OPLL. The ossified posterior longitudinal ligament behind the C-2

TABLE 1: Clinical data for 5 patients with OPLL*

Parameter	Case 1	Case 2	Case 3	Case 4	Case 5	Mean
age (yrs)	43	64	71	65	71	63
duration of follow-up monitoring (yrs)	3.6	2.6	3.5	2.1	3.8	3.1
JOA score (preop/postop)	7.5/15.5	9.5/17	8.5/15	6.5/14.5	10.5/16	8.5/15.6
OPLL type	mixed	localized	mixed	mixed	mixed	
progression length (mm)	8.9	6.4	3.6	2.5	2.1	4.7
progression rate (mm/yr)	2.4	2.5	1.0	1.2	0.6	1.5
vol increase (mm^3)	3851	369	2139	728	1022	1622
vol increase rate (mm^3/yr)	1056	143	608	346	268	484
expansion rate (%)	89	40	22	15	18	37

* JOA = Japanese Orthopaedic Association.

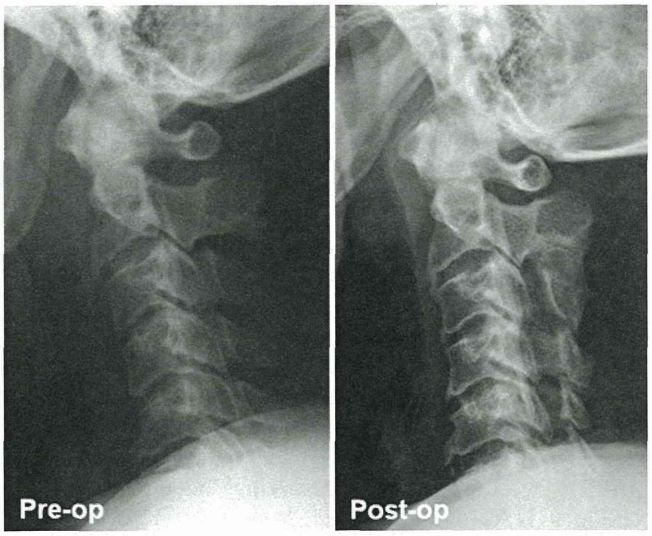

FIG. 3. Case 1. Plain lateral radiographs showing the mixed type of OPLL with the continuous type at C2–3 and the segmental type below C-2. However, it was difficult to recognize the segmental type of OPLL below the C-4 level on the preoperative radiograph.

vertebra had grown 8.9 mm cranially, and the volume increase was 769 mm^3. The ossified posterior longitudinal ligament of the C-4 vertebra had expanded; the volume increase was 977 mm^3. However, there was little progression in the C2–3 intervertebral space, which had already fused and had little mobility before surgery. The segmental type of OPLL at the C-6 level had grown only 1.2 mm, with a volume increase of 129 mm^3. Meanwhile, the segmental type of OPLL of the C-7 vertebra had grown 7.2 mm, with a volume increase of 708 mm^3. There was a big difference in growth between ossifications.

Case 2

This 64-year-old man with a localized type OPLL

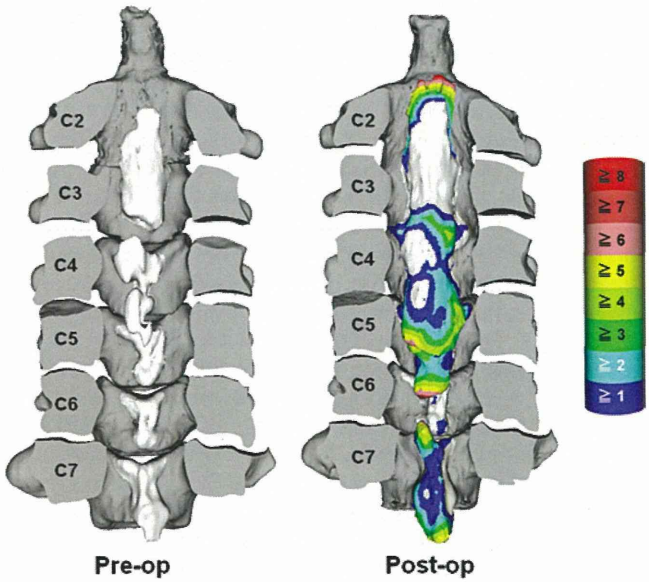

FIG. 4. Case 1. Three-dimensional models. The *bar* at the right shows the relationship between progression length and color.

TABLE 2: Accuracy of voxel-based registration of the cervical spine

Position	Rx (°)	Ry (°)	Rz (°)	Tx (mm)	Ty (mm)	Tz (mm)
1	0.26	0.08	−0.03	0.13	0.00	0.36
2	0.22	0.14	−0.11	−0.13	0.16	−0.30
3	0.06	0.08	0.29	0.10	0.03	0.41
4	−0.10	0.04	-0.28	0.02	0.07	−0.07
5	0.00	0.16	-0.09	0.13	−0.10	0.08
6	−0.21	−0.10	0.32	−0.17	0.34	0.14
7	−0.29	−0.25	−0.18	0.01	−0.05	0.58
8	0.17	0.08	−0.24	−0.19	0.12	−0.13
RMSE	0.19	0.13	0.21	0.13	0.15	0.31

* Rx = flexion-extension; Ry = axial rotation; Rz = lateral bending; Tx = lateral translation; Ty = superoinferior translation; Tz = anteroposterior translation.

underwent surgery. It was difficult to recognize OPLL on preoperative radiography (Fig. 5). However, CT scanning clearly revealed the OPLL attached to the C-4 vertebra (Fig. 6). Two years after laminoplasty, the OPLL had grown 6.4 mm in the cranial direction, with a volume increase of 369 mm^3.

Discussion

Advantages of CT Evaluation

Although several studies have reported on progression of OPLL, 2D evaluation with plain lateral radiographs has some limitations. Three-dimensional evaluation with CT scanning is better suited to measuring OPLL growth. For example, in the lower cervical spine, OPLL is likely to be masked by the shoulder girdle shadows. In young patients, OPLL may be less distinct because the ossification is less densely calcified. Although growth can occur in any direction, only craniocaudal and ventrodorsal progression are depicted on plain radiographs. Growth in the oblique direction is projected only orthographically onto a radiograph. Compared with radiography, CT scanning has several advantages. Computed tomography scanning is the most sensitive diagnostic method for detecting small ossifications or calcifications of the ligament, which are likely to be missed on radiographs.[15] However, conventional CT scanning also has the limitation of slice thickness. Measurement of OPLL on conventional radiographs is unreliable because the slice is likely to be thick, owing to the limited number of films used. It is also difficult to slice OPLL on the same level and angle to compare past and present

TABLE 3: Intraobserver reproducibility of volume measurement

Observer	ICC (95% CI)	RMSE (mm^3)	CV (%)
1	0.992 (0.970–0.998)	10.7	1.0
2	0.980 (0.928–0.995)	17.3	2.1
3	0.990 (0.962–0.998)	20.0	1.9
mean	0.987 (0.953–0.997)	16.0	1.7

TABLE 4: Interobserver reproducibility of volume measurement

Measurement	ICC (95% CI)	RMSE (mm^3)	CV (%)
1st	0.956 (0.842–0.989)	39.2	4.1
2nd	0.980 (0.919–0.995)	27.1	2.7
mean	0.968 (0.880–0.992)	33.1	3.4

ossification. However, these limitations can be overcome using helical scanning with multidetector CT and digital viewers. Additionally, accurate superimposition by voxel-based registration facilitates comparison of OPLL before and after surgery. The Orthopedic Viewer that we used was developed specifically for our study; however, the program was written using Visualization Toolkit (http://www.vtk.org/), an open-source free software system. Therefore, the measurement method that we used can be universally applied using similar viewers with equivalent function.

In our study, 3D evaluation, including volume increase, depicted minor changes in OPLL with high sensitivity. Hori et al.[5,6] reported that progression of greater than 2 mm on a plain radiograph occurred in 56.5%–75% of patients 2 years after laminoplasty. However, our method revealed that progression of greater than 0.5 mm occurred in all patients and that the mean rate of volume increase was 484 mm^3/year. Despite the growth of OPLL, myelopathy did not worsen in any patient in our study, partly because decompression was enough to forestall it. If enough space for the spinal cord can be obtained through laminoplasty, the growth of ossification could help decrease the dynamic factor and might not always be a clinical problem. However, the growth of OPLL after surgery could be a cause for revision surgery in some cases.[4,11,21] Fujiyoshi et al.[3] reported that additional fusion for mobile segments in laminoplasty could slow the progression of OPLL. Ono et al.[16] reported that etidronate disodium had the potential to slow progression. Because OPLL is a kind of ectopic bone formation, some inhibitors of bone formation can prevent OPLL growth. It is essential to have an accurate and reliable measurement method to determine the efficacy of such drugs or of surgical procedures to decrease growth. The method that we used can be a useful tool for the future study of the natural progression process or the efficacy of drugs or surgery in treating OPLL.

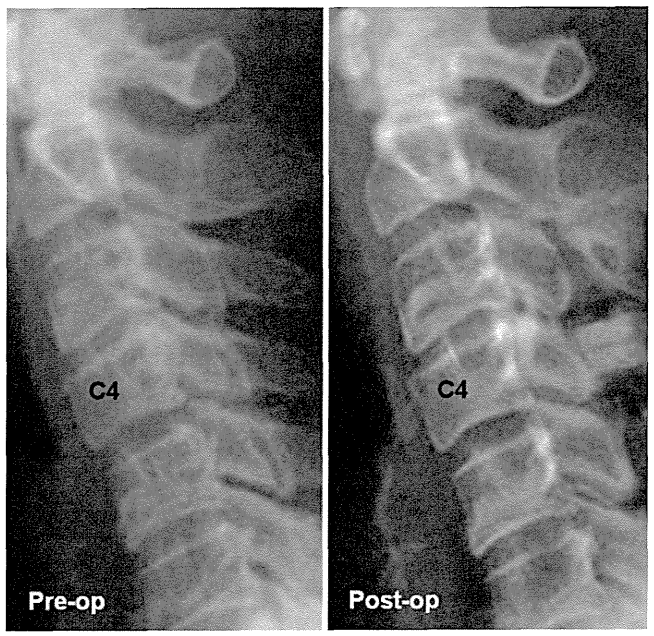

FIG. 5. Case 2. Plain lateral radiographs showing the localized type of OPLL at C-4. It was difficult to recognize ossification on the preoperative radiograph **(left)**. The postoperative radiograph **(right)** shows ossification; however, the length of progression was unclear.

Factors in Ossification Growth

Factors in ossification growth are roughly classified as either general or local. General factors include age, sex, and some hormonal factors, such as genetics, growth factors, and cytokines. It has been reported that collagen 11A2, collagen 6A1, bone morphogenetic protein–2, and transforming growth factor–β are related to progression of OPLL.[18,19] Local factors include mechanical stress, types of OPLL, and types of surgical procedures. Some researchers have reported that the segmental type of OPLL does not progress much in general.[2,5] Chiba et al.[2] reported that progression occurred in 53.3% of the continuous type of OPLL, 27.3% of the segmental type, 67.3% of the mixed type, and 40% of the localized type. They noted that the incidence of progression was significantly higher in patients younger than 59 years than in those older than 60 years. Hori et al.[5] reported that longitudinal progression occurred in 85% of the continuous type of OPLL, 29% of the segmental type, 100% of the mixed type, and 100% of the localized type. They also reported that thickening of ossifications occurred in 38% of the continuous type of OPLL, 0% of the segmental type, 41% of the mixed type, and 0% of the localized type.[6] They speculated that the pathological entity might be different for the continuous or mixed type of OPLL versus the segmental type. However, some reports of studies with longer follow-up periods noted that the segmental type of OPLL went on to become the continuous or mixed type of OPLL.[14,20] Murakami et al.[14] reported that the segmental type of OPLL had become the continuous type by 10 years of follow-up. They argued that the segmental type of OPLL was an initial stage of the continuous or the mixed type and that the entity was not different. Our findings correspond with those of Murakami et al.; however, we found that the extent of growth between OPLL types was considerably different even in the same patient (Case 1). It is not easy to explain these differences, because the growth process is not influenced by a single factor. However, one of the possible reasons for this is that the segmental type of OPLL located at the middle of a vertebral body grows slowly because it is not subjected to dynamic factors to the extent that OPLL in other locations is affected. Once the tip of an ossification reaches the intervertebral area, growth may be activated by increased dynamic factors. Hirabayashi et al.[4] reported that pseudarthrosis-like thickening occurred at mobile intervertebral spaces and that these changes stopped only after elimination of mobility. Our results correspond with theirs. In our study, ossifications grew actively in inter-

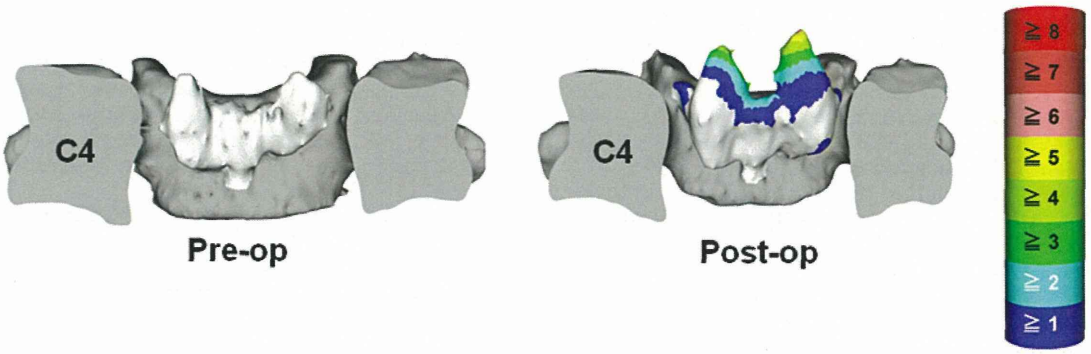

FIG. 6. Case 2. Three-dimensional models. The *bar* at the right shows the relationship between progression length and color.

vertebral areas as if they were bridging gaps to stabilize the mobile segments (Fig. 4). This finding suggests that dynamic factors are strongly involved in growth.[13] We speculate that the growth of OPLL decreases with the stabilizing effect of ossifications themselves and of laminoplasty.

In discussing the reasons for the different growth rates in different types of OPLL, the problem is the difficulty of detecting OPLL at its onset. A small ossification in the initial stage may sometimes be accidentally found, but most ossifications are found at a mature stage because a certain level of ossification must usually be attained before patients experience symptoms. Many studies have reported that ossifications do not grow at a constant speed but instead have growth spurts.[5,20] Therefore, it is theoretically possible that the mixed type of OPLL may be a form of the activated phase of the OPLL growth process. To answer these questions, long-term observation of OPLL starting from the initial stage is necessary. Our accurate 3D evaluation method can be an appropriate tool for further observation.

Conclusions

A novel 3D method for measuring OPLL growth, involving scanning by multidetector CT, showed that progression of greater than 0.5 mm occurred in all patients. After laminoplasty, the mean maximum progression rate was 1.5 mm/year, and the mean volume increase rate was 484 mm^3/year. This method can accurately detect changes in OPLL and thus can be a useful, reliable tool for examining OPLL growth.

Disclosure

This work was supported by a grant-in-aid from the Investigation Committee on Ossification of the Spinal Ligaments, Japanese Ministry of Public Health, Labor, and Welfare and a grant-in-aid for Scientific Research C (KAKENHI:22591632) from the Japan Society for the Promotion of Science. No benefits in any form have been or will be received from a commercial party related directly or indirectly to the subject of this manuscript.

Author contributions to the study and manuscript preparation include the following. Conception and design: Fujimori, Iwasaki, Ishii. Acquisition of data: Fujimori, Iwasaki. Analysis and interpretation of data: Fujimori, Nagamoto. Drafting the article: Fujimori. Critically revising the article: all authors. Reviewed submitted version of manuscript: all authors. Approved the final version of the manuscript on behalf of all authors: Fujimori. Statistical analysis: Fujimori. Administrative/technical/material support: Iwasaki, Yoshikawa, Sugamoto. Study supervision: Iwasaki, Yoshikawa, Sugamoto.

Acknowledgments

The authors thank Aya Sasaki. Katharine O'Moore-Klopf, E.L.S. (East Setauket, NY) provided professional English-language editing of this article.

References

1. Chiba K, Kato Y, Tsuzuki N, Nagata K, Toyama Y, Iwasaki M, et al: Computer-assisted measurement of the size of ossification in patients with ossification of the posterior longitudinal ligament in the cervical spine. **J Orthop Sci 10:**451–456, 2005
2. Chiba K, Yamamoto I, Hirabayashi H, Iwasaki M, Goto H, Yonenobu K, et al: Multicenter study investigating the postoperative progression of ossification of the posterior longitudinal ligament in the cervical spine: a new computer-assisted measurement. **J Neurosurg Spine 3:**17–23, 2005
3. Fujiyoshi T, Yamazaki M, Okawa A, Kawabe J, Hayashi K, Endo T, et al: Static versus dynamic factors for the development of myelopathy in patients with cervical ossification of the posterior longitudinal ligament. **J Clin Neurosci 17:**320–324, 2010
4. Hirabayashi K, Miyakawa J, Satomi K, Maruyama T, Wakano K: Operative results and postoperative progression of ossification among patients with ossification of cervical posterior longitudinal ligament. **Spine (Phila Pa 1976) 6:**354–364, 1981
5. Hori T, Kawaguchi Y, Kimura T: How does the ossification area of the posterior longitudinal ligament progress after cervical laminoplasty? **Spine (Phila Pa 1976) 31:**2807–2812, 2006
6. Hori T, Kawaguchi Y, Kimura T: How does the ossification area of the posterior longitudinal ligament thicken following cervical laminoplasty? **Spine (Phila Pa 1976) 32:**E551–E556, 2007
7. Hsieh PC, Wang MY: Introduction. Ossification of the posterior longitudinal ligament. **Neurosurg Focus 30(3):**Introduction, 2011
8. Inoue S, Goto S, Nagase J, Tanaka Y: Investigation of window width and window level of computed tomography for OPLL, in: **Annual Report of Taskforce of Research for Ossification of the Spinal Ligaments.** Tokyo: Japanese Ministry Of Public Health and Welfare, Vol 58, 1984, pp 237–239
9. Ishii T, Mukai Y, Hosono N, Sakaura H, Nakajima Y, Sato Y, et al: Kinematics of the upper cervical spine in rotation: in vivo three-dimensional analysis. **Spine (Phila Pa 1976) 29:** E139–E144, 2004
10. Iwasaki M, Kawaguchi Y, Kimura T, Yonenobu K: Long-term

results of expansive laminoplasty for ossification of the posterior longitudinal ligament of the cervical spine: more than 10 years follow up. **J Neurosurg 96 (2 Suppl):**180–189, 2002
11. Kawaguchi Y, Kanamori M, Ishihara H, Nakamura H, Sugimori K, Tsuji H, et al: Progression of ossification of the posterior longitudinal ligament following en bloc cervical laminoplasty. **J Bone Joint Surg Am 83-A:**1798–1802, 2001
12. Kokubun S, Sato T, Nishihira T: Computed tomography of the ossification of the spinal ligaments, in: **Seikeigeka Mook.** Tokyo: Kanehara Shuppan, Vol 50, pp 59–71, 1987
13. Matsunaga S, Sakou T, Taketomi E, Nakanisi K: Effects of strain distribution in the intervertebral discs on the progression of ossification of the posterior longitudinal ligaments. **Spine (Phila Pa 1976) 21:**184–189, 1996
14. Murakami M, Seichi A, Chikuda H, Takeshita K, Nakamura K, Kimura A: Long-term follow-up of the progression of ossification of the posterior longitudinal ligament. Case report. **J Neurosurg Spine 12:**577–579, 2010
15. Nagata K, Sato K: Diagnostic imaging of cervical ossification of the posterior longitudinal ligament, in Yonenobu K, Nakamura K, Toyama Y (eds): **OPLL: Ossification of the Posterior Longitudinal Ligament, ed 2.** Tokyo: Springer, 2006, pp 127–143
16. Ono K, Yonenobu K, Sako T, Kawai S, Nagata K: [Prevention of progression of ossification of the posterior longitudinal ligament (OPLL) by the administration of etidronate disodium (EHDP) after posterior decompression.] **Nippon Sekitsui Geka Gakkai Zasshi 9:**432–442, 1998 (Jpn)
17. Saetia K, Cho D, Lee S, Kim DH, Kim SD: Ossification of the posterior longitudinal ligament: a review. **Neurosurg Focus 30(3):**E1, 2011
18. Stapleton CJ, Pham MH, Attenello FJ, Hsieh PC: Ossification of the posterior longitudinal ligament: genetics and pathophysiology. **Neurosurg Focus 30(3):**E6, 2011
19. Stetler WR, La Marca F, Park P: The genetics of ossification of the posterior longitudinal ligament. **Neurosurg Focus 30(3):** E7, 2011
20. Terayama K, Ohtsuka K, Tsuama N, Ohtani K, Yamauchi Y, Yamaura I, et al: Investigation of ossification of the spinal ligaments with more than 5 years follow-up, in: **Annual Report of Taskforce of Research for Ossification of the Spinal Ligaments.** Tokyo: Japanese Ministry Of Public Health and Welfare, Vol 58, 1984, pp 85–96
21. Tokuhashi Y, Ajiro Y, Umezawa N: A patient with two resurgeries for delayed myelopathy due to progression of ossification of the posterior longitudinal ligaments after cervical laminoplasty. **Spine (Phila Pa 1976) 34:**E101–E105, 2009

Manuscript submitted June 2, 2011.
Accepted November 7, 2011.
Please include this information when citing this paper: published online December 16, 2011; DOI: 10.3171/2011.11.SPINE11502.

Address correspondence to: Takahito Fujimori, M.D., Department of Orthopedic Surgery, Osaka University Graduate School of Medicine, 2-2 Yamadaoka, Suita, Osaka 565-0871, Japan. email: takahito-f@hotmail.co.jp.

J Neurosurg Spine 17:74–81, 2012

Three-dimensional measurement of intervertebral range of motion in ossification of the posterior longitudinal ligament: are there mobile segments in the continuous type?

Clinical article

Takahito Fujimori, M.D.,[1] Motoki Iwasaki, M.D., Ph.D.,[1] Yukitaka Nagamoto, M.D.,[1] Masafumi Kashii, M.D., Ph.D.,[1] Takahiro Ishii, M.D., Ph.D.,[2] Hironobu Sakaura, M.D., Ph.D.,[3] Kazuomi Sugamoto, M.D., Ph.D.,[4] and Hideki Yoshikawa, M.D., Ph.D.[1]

Departments of [1]Orthopedic Surgery and [4]Orthopedic Biomaterial Science, Osaka University Graduate School of Medicine; [2]Department of Orthopedic Surgery, Kaizuka City Hospital, Osaka; and [3]Department of Orthopedic Surgery, Kansai Rosai Hospital, Hyogo, Japan

Object. In this paper, the authors' goals were to determine the extent of the effect of continuous-type ossification of the posterior longitudinal ligament (OPLL) of the cervical spine on intervertebral range of motion (ROM) and to examine the relationship between the 3D morphology of OPLL and intervertebral ROM.

Methods. The authors evaluated 5 intervertebral segments in each of 20 patients (11 men and 9 women) with continuous-type OPLL, for a total of 100 intervertebral segments, using functional CT in anteroposterior (AP) flexion and right and left axial rotation. Three-dimensional kinematics were evaluated using the voxel-based registration method. Ossification was classified on the basis of 3D kinematics and morphology.

Results. The authors found 49 ossifications that were obviously of the continuous type. They were divided into 2 types: 1) bridging (13 instances), with thick, continuous ossification of the anterior or posterior longitudinal ligament bridging intervertebral segments and with an ROM of 0.3° in AP flexion and 0.2° in rotation; and 2) nonbridging (36 instances), with a minute gap in the ossification itself or between the ossification and vertebra and with an ROM of 4.9° in AP flexion and 4.0° in rotation. There were 8 stalagmite-type ossifications in the nonbridging group that had the unique kinematics of restricted AP flexion and normal axial rotation.

Conclusions. The authors' findings indicate that most continuous-type ossifications that are categorized using the conventional radiographic classification system have mobile segments. The discrimination between bridging and nonbridging on CT scans can be a useful predictive index for dynamic factors.
(http://thejns.org/doi/abs/10.3171/2012.3.SPINE111083)

Key Words • **computed tomography** • **range of motion** • **ossification of the posterior longitudinal ligament** • **bridging-type ossification** • **in vivo 3D imaging** • **cervical spine**

Ossification of the posterior longitudinal ligament of the cervical spine is one of the causes of cervical myelopathy. Tsuyama[18] classified the types of ossification, as seen on lateral radiographs, as continuous, segmental, mixed, and localized (Fig. 1). Both static compression and dynamic factors are considered to be related to the deterioration of myelopathy.[1,4,7,8,10–15] Matsunaga et al.[11] based the importance of dynamic factors on the fact that all patients with a relatively large OPLL do not develop myelopathy. However, it is unknown to what extent dynamic factors interact with static compression in the deterioration of myelopathy. There is still controversy about how to define dynamic factors. Some researchers have reported that total ROM is significantly larger in patients with myelopathy than in those without myelopathy and that a large total ROM is thus a risk factor.[11,14] How-

Abbreviations used in this paper: AP = anteroposterior; JOA = Japanese Orthopaedic Association; OPLL = ossification of the posterior longitudinal ligament; ROM = range of motion.

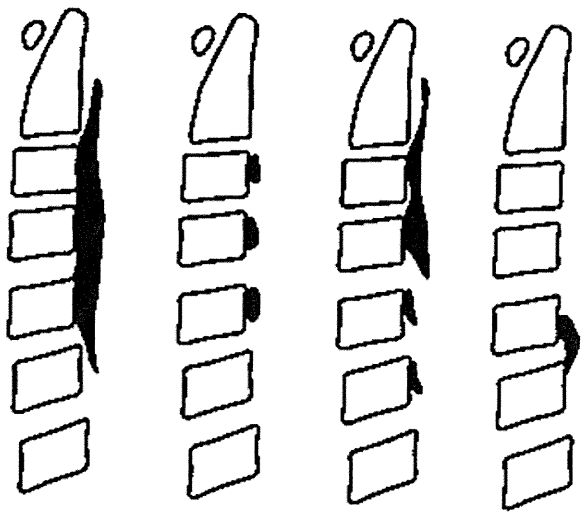

FIG. 1. The morphology of ossification based on lateral radiographs.

ever, Morio et al.[15] reported that there is no significance in total ROM between patients with myelopathy and those without it. They emphasized that the intervertebral ROM at the level responsible for myelopathy was important. Actually, in many cases, the stenosis site does not necessarily correspond to the area of abnormal mobility. Even when the stenosis site coincides with the mobile segment it is often difficult to quantify the small intervertebral ROM on functional radiography. The reliable measurable angle was approximately 3° on plain radiographs.[3,5,17]

Continuous-type OPLL was reported to have a better prognosis than mixed-type OPLL because it was erroneously believed that continuous-type OPLL is not capable of much motion.[11] However, findings on AP plain radiographs suggest that continuous-type OPLL also has some sort of motion as a whole. We conducted a study to examine the dynamic factor at each segment of continuous-type OPLL. The purpose of our study was first to measure the intervertebral ROM in continuous-type ossification and second to examine the relationship between the intervertebral ROM and the 3D morphology of ossification.

Methods

Our study participants were 20 patients with cervical OPLL who visited our facility between June 2009 and June 2010, not necessarily for their first visit. All study protocols were approved by our institution's review board. The study group included 11 men and 9 women with an average age of 64.5 years (range 40–78 years). The average JOA score was 14.7; the maximum possible score on the scale is 17. The inclusion criterion was the presence of continuous-type or mixed-type (combination of continuous-type and segmental-type) ossification, documented by plain lateral radiographs. Patients with only segmental ossification and those who had previously undergone cervical spinal surgery were excluded. Patients with moderate to severe myelopathy (JOA score < 11) were also excluded because posterior flexion could increase their myelopathy. Five intervertebral ROM measurements were obtained for each patient: C2–3, C3–4, C4–5, C5–6, and C6–7; thus, ROM was measured for a total of 100 intervertebral segments. To find obvious instances of continuous-type ossification, 4 spine surgeons evaluated radiographs of all ossifications. Only if all 4 surgeons agreed that the ossification was continuous was it included in the study.

Measurement of Intervertebral ROM

Low-dose functional CT scans were obtained for 5 positions for each patient using a commercial CT system (LightSpeed, GE Healthcare) with the following parameters: slice thickness 0.625 mm; pixel size 0.352 mm; tube rotation speed 0.5 seconds; beam collimation 40 mm; beam pitch 0.9; tube current 50 mA; voltage 120 kV. Patients were placed supine on the CT table in neutral position, at maximum AP flexion and maximum axial rotation to the left and right achievable without pain or discomfort. A supportive device was used to keep the head in anterior flexion. Patients were instructed to rotate their head as perpendicularly as possible to the axis of their body trunk, and their shoulders were horizontally fixed to the table with belts (Fig. 2). The ROM for AP flexion was calculated as the sum of the anterior flexion and the posterior flexion angle, and the ROM of axial rotation was calculated as the sum of the right rotation angle and the left rotation angle.

To reduce radiation exposure, scans done in positions other than neutral were performed with a lower tube current: 15 mA for rotation and posterior flexion and 30 mA only for anterior flexion to reduce artifact of the jawbone. Total exposure was 90 dose-length products, which is less than that specified for routine CT scanning by our hospital. The CT data were transferred via a DICOM (Digital Imaging and Communications in Medicine) network into a computer workstation, where image processing was performed using Virtual Place software (M series, Medical Imaging Laboratory). First, each vertebra was semiautomatically extracted using a process known as segmentation. A bone window with a width of 2000 HU and a level of 150 HU was used for the threshold, as has been done in earlier studies.[6] Second, the segmented vertebrae in the neutral position were superimposed on other positions using a process known as voxel-based registration. Voxel-based registration is an accurate method for determining the relative positions of 3D models at different coordinates, using a corresponding method that is based on the correlation between CT values of each voxel. This calculation is performed using software, and the relative positions are represented as a matrix. This matrix is converted to 6 df by Euler angles, with the sequence of yaw (Y), pitch (X), roll (Z), and translations, using a previously defined coordinate system.[16] As part of our study, we validated the accuracy of this method for CT scanning of the cervical spine. We performed in vitro validation of the accuracy of our experimental CT method for the cervical spine using fresh-frozen vertebrae. More than 8 tantalum beads with a radius of 1.0

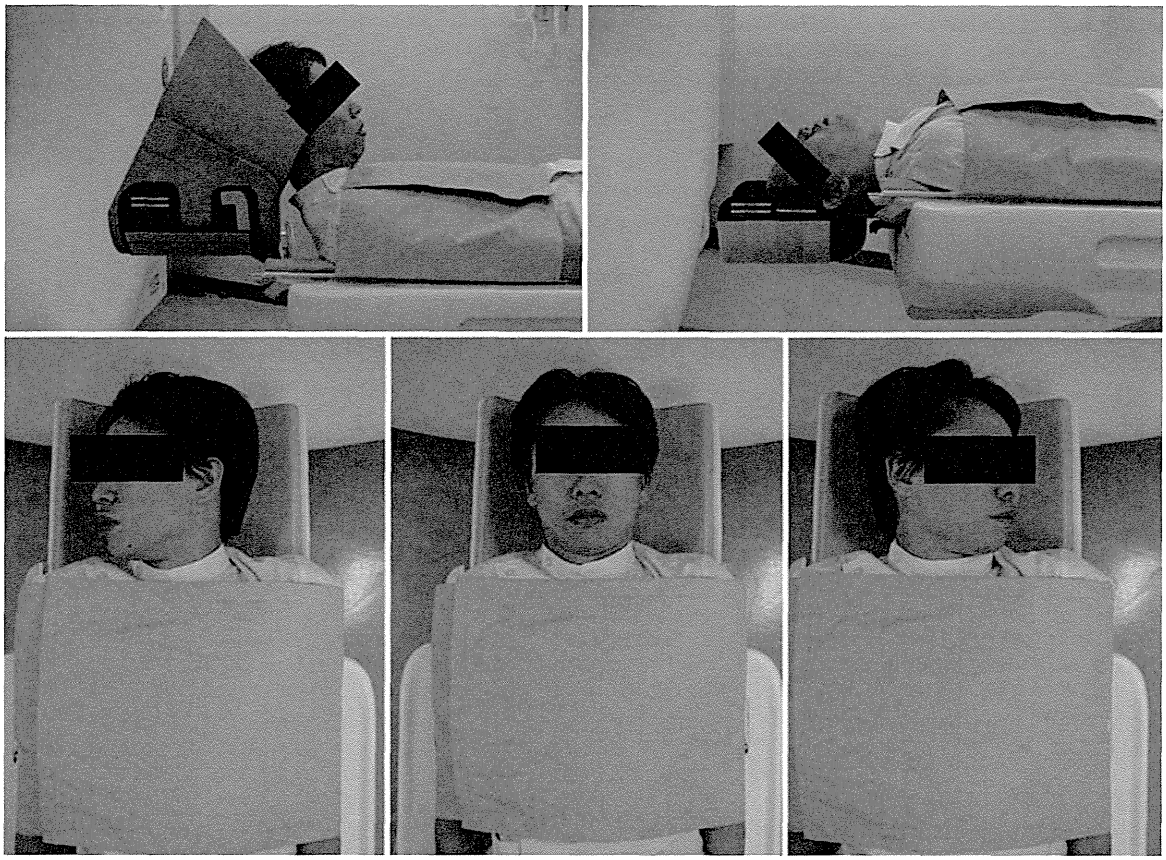

FIG. 2. Acquisition of CT scans of maximum AP flexion and maximum axial rotation. The examiner was instructed to help participants bend their necks until they could rest their chin on their chest with the use of a supportive device in anterior flexion without pain or discomfort, and to have participants rotate their head perpendicular to the axis of their body trunk.

mm were implanted in the vertebrae. Subsequently, CT scans were obtained 8 times in different positions with the same imaging parameters. Each vertebra was then superimposed by voxel-based registration. The true value of the migration was measured using marker-based registration, providing gold-standard data, and accuracy was defined as the closeness to the true value (Table 1). The root mean square distance was 0.19° in flexion-extension, 0.13° in axial rotation, 0.21° in lateral bending, 0.13 mm in lateral translation, 0.15 mm in superoinferior translation, and 0.31 mm in AP translation, demonstrating that voxel-based registration enabled far more accurate measurement than radiography.

Morphological Pattern of Ossification

The ossification pattern was classified on the basis

TABLE 1: Accuracy of voxel-based registration of the cervical spine*

Position	Rx (°)	Ry (°)	Rz (°)	Tx (mm)	Ty (mm)	Tz (mm)
1	0.26	0.08	−0.03	0.13	0.00	0.36
2	0.22	0.14	−0.11	−0.13	0.16	−0.30
3	0.06	0.08	0.29	0.10	0.03	0.41
4	−0.10	0.04	−0.28	0.02	0.07	−0.07
5	0.00	0.16	−0.09	0.13	−0.10	0.08
6	−0.21	−0.10	0.32	−0.17	0.34	0.14
7	−0.29	−0.25	−0.18	0.01	−0.05	0.58
8	0.17	0.08	−0.24	−0.19	0.12	−0.13
RMSE	0.19	0.13	0.21	0.13	0.15	0.31

* RMSE = root mean square error; Rx = flexion-extension; Ry = axial rotation; Rz = lateral bending; Tx = lateral translation; Ty = superoinferior translation; Tz = anteroposterior translation.

of 3D continuity between the ossification and the vertebra, as well as the ossification itself. All reconstructed sagittal slices with a thickness of 0.625 mm were examined on the digital viewer (AquariusNET client viewer, TeraRecon, Inc.). To perform an accurate assessment of ROM and ossification pattern, ossification of both the anterior and posterior longitudinal ligaments was covered as observation objects. The relationship between intervertebral ROM and the morphology of ossification was examined. The unpaired t-test was used for statistical analysis as appropriate with JMP software (version 8.0.1, SAS Institute). Probability values < 0.05 were considered to indicate statistical significance.

Results

Range of Motion of Intervertebral Segments

The average ROM of the 100 intervertebral segments was 7.3° in AP flexion and 3.5° in axial rotation. In those 100 intervertebral segments, continuous ossification was apparent on plain radiographs in 49 intervertebral segments. The average ROM for those segments was 3.7° in AP flexion and 3.0° in axial rotation (Table 2).

Computed Tomography Classification Based on In Vivo 3D Kinematics

Bridging and Nonbridging Ossification. We divided these 49 continuous-type ossifications into 2 groups on the basis of thin-sliced reconstructed sagittal CT scanning: bridging (Fig. 3A) with thick, continuous ossification of the anterior and/or posterior longitudinal ligament bridging intervertebral segments with bony union, and nonbridging (Fig. 3B), in which there is a minute gap in ossification itself or between the ossification and the vertebra. There were 13 bridging (27%) and 36 nonbridging (73%) ossifications. The intervertebral ROM of bridging ossifications was 0.3° in AP flexion and 0.2° in axial rotation; the respective values for nonbridging ossifications were 4.9° and 4.0° in axial rotation (Table 2). The bridging type had a significantly smaller intervertebral ROM than did the nonbridging type both in AP flexion and in axial rotation ($p < 0.001$), as shown in Video 1.

Video 1. Video clip showing 3D motion of bridging **(left)** and nonbridging **(right)** type of ossifications. Video shows that the bridging type has little motion in anteroposterior flexion and axial rotation. However, the nonbridging type has a comparatively large intervertebral range of motion. Used with permission from Takahito Fujimori. Click here to view with Media Player. Click here to view with Quicktime.

About half of the continuous ossifications were of the bridging type at the C5–6 and C6–7 levels. However, most of the continuous ossifications at the C2–3, C3–4, and C4–5 levels were of the nonbridging type. Of the 13 bridging ossifications, 10 accompanied bridging of ossification of the anterior longitudinal ligament at the same segments.

Stalagmite-Type Ossification. Among the nonbridging ossifications, 1 type had a characteristic intervertebral ROM. There was limited AP flexion and normal axial rotation in the ossifications originating from the lower vertebra and progressing continuously through and behind the upper vertebral body without contact (Fig. 3C), as shown in Videos 2 and 3.

TABLE 2: The mean intervertebral ROM of each type of ossification*

Type of Ossification	Total	Radiographically Continuous	Bridging	Nonbridging
no. of intervertebral segments	100	49	13	36
AP flexion (°)†	7.3 ± 5.6	3.7 ± 4.0	0.3 ± 0.3	4.9 ± 4.5
rotation (°)‡	3.5 ± 2.8	3.0 ± 2.9	0.2 ± 0.3	4.0 ± 2.7

* Mean values are presented as the mean ± SDs.
† Sum of anterior and posterior flexion angles.
‡ Sum of right and left rotation angles.

Video 2. Video clip showing 3D motion of the stalagmite type of ossification in anteroposterior flexion. Stalagmite-type ossifications have restricted anteroposterior flexion. Used with permission from Takahito Fujimori. Click here to view with Media Player. Click here to view with Quicktime.

Video 3. Video clip showing 3D motion of the stalagmite type of ossification in axial rotation. Stalagmite-type ossifications have normal axial rotation. Used with permission from Takahito Fujimori. Click here to view with Media Player. Click here to view with Quicktime.

We named these "stalagmite-type ossifications" because they grow slowly upward like the geologic formations. There were 8 stalagmite ossifications with an average intervertebral ROM of 1.6° in AP flexion and 4.6° in axial rotation. In comparison, the other 28 nonbridging, nonstalagmite ossifications had an average 5.9° of AP flexion and 3.9° of axial rotation. The stalagmite ossifications had significantly smaller AP flexion ($p < 0.05$) but normal axial rotation compared with the other nonbridging ossifications. All stalagmite ossifications occurred at the C2–3 or C3–4 level.

Relationship Between Neurological Symptom and Type of Ossification

We retrospectively analyzed the JOA scores of 13 patients who were monitored for more than 2 years. There were 2 patients in the bridging group whose ossifications were all bridging; the other 11 patients in the nonbridging group had at least 1 nonbridging ossification. The mean change in JOA score during the follow-up period was 0.3 points/18.5 years in the bridging group and −0.5 points/8.6 years in the nonbridging group. These results suggest that neurological function was maintained for long periods in the bridging group but that deterioration tended to occur in the nonbridging group.

Illustrative Cases

Case 1

Plain radiographs obtained in this 55-year-old woman showed apparent continuous-type ossifications; however,